ISSN 0036-0236, Russian Journal of Inorganic Chemistry, 2013, Vol. 58, No. 10, pp. 1220–1226. © Pleiades Publishing, Ltd., 2013.
Original Russian Text © A.Yu. Chufarov, N.A. Forostyanaya, A.N. Ermakov, R.F. Samigulina, L.N. Maskaeva, V.F. Markov, Yu.G. Zainulin, 2013, published in Zhurnal Neorganicheskoi Khimii, 2013, Vol. 58, No. 10, pp. 1362–1369.

PHYSICAL METHODS OF INVESTIGATION

Phase Formation and Structural Characteristics of Cd–Pb–S Nanopowder Compositions Produced by Modification of CdS Powder in a Citrate–Ammonia Solution of a Lead Salt

A. Yu. Chufarov[a], N. A. Forostyanaya[b], A. N. Ermakov[a, b], R. F. Samigulina[a], L. N. Maskaeva[b], V. F. Markov[b], and Yu. G. Zainulin[a]

[a] *Institute of Solid-State Chemistry, Ural Branch, Russian Academy of Sciences, ul. Pervomaiskaya 91, Yekaterinburg, 620041 Russia*

[b] *Ural Federal University named after the First President of Russia B.N. Eltsyn, ul. Mira 19, Yekaterinburg, 620002 Russia*

Received December 27, 2012

Abstract—Nanopowders obtained by modification of a cadmium sulfide powder in a citrate–ammonia solution of lead acetate have been studied by X-ray diffraction, electron microscopy, and thermal analysis. The type of crystal structure and composition of Cd–Pb–S nanopowders depend on the conditions of their synthesis. The thermoanalytical curves show a well-defined endotherm in the temperature range 284–321°C. The position of this endotherm depends on the duration of contact of a CdS powder with an aqueous solution of a lead salt. Heating nanopowders to 600°C in an argon flow leads to formation of oxygen-containing phases: lead sulfate and cadmium oxide.

DOI: 10.1134/S0036023613100057

Compounds of variable composition in the CdS–PbS system are important photoelectric and luminescent materials. At the same time, cadmium sulfide, exhibiting a unique sensitivity to visible light, has low degradation and radiation resistance. This disadvantage can be mitigated by introducing narrow-gap lead sulfide into the CdS structure [1–3]. Simultaneously, polycrystalline layers based on the heterophase CdS–PbS material exhibit much better photosensitivity, which is a decisive factor of its use as efficient functional elements in opto- and nanoelectronics.

It is worth noting that lead and cadmium sulfides have limited mutual solubilities. In particular, according to the high-temperature phase diagram, the PbS solubility in cadmium sulfide at 1203 K is less than 0.1 mol % [4]. CdS–PbS compounds are mainly produced by thermal evaporation [5].

To extend the application of the heterophase material based on cadmium sulfide modified with lead sulfide, new methods of synthesis of Cd–Pb–S compounds should be developed. Films of $Cd_{1-x}Pb_xS$ solid solutions have been fabricated through ion exchange substitution of lead ions for cadmium ions in the CdS film–aqueous lead salt solution system by keeping a freshly deposited cadmium sulfide film (obtained by chemical deposition) in a lead acetate solution [6]. It is of interest to use cadmium sulfide nanopowders, which have essentially different properties, in analogous studies.

The present work is aimed at fabrication of Cd–Pb–S nanopowders by modifying a CdS powder in a citrate–ammonia solution of a lead salt and study of structural, phase, and morphological transformations at high temperatures.

EXPERIMENTAL

The procedure of preparation of Cd–Pb–S nanopowder compositions consisted in treating the cadmium sulfide powder with a lead acetate solution. CdS powder was synthesized by chemical deposition by mixing stoichiometric amounts of aqueous solutions of cadmium chloride $CdCl_2$, sodium citrate $Na_3C_6H_5O_7$, ammonium hydroxide NH_4OH, and thiourea CSN_2H_4. The resulting yellow-orange powders were kept for 1–10 h at 333–368 K in an aqueous ammonia solution of lead acetate $Pb(CH_3COO)_2$ containing sodium citrate as a complexing agent. After this treatment, the powders acquired a light grey color typical of lead sulfide. The change in color indicated that lead was incorporated in the cadmium sulfide powder. Alkalization of the solution with ammonia, which acts as a ligand for cadmium, is favorable for endocrypty (entrapment) and incorporation of a minor element in the structure of the host crystal owing to the establishment of a forced equilibrium at the CdS_s/Pb^{2+}_{soln} interface [7].

The structural and morphological characteristics and the phase and elemental composition of nanopowders were studied by X-ray diffraction, scanning

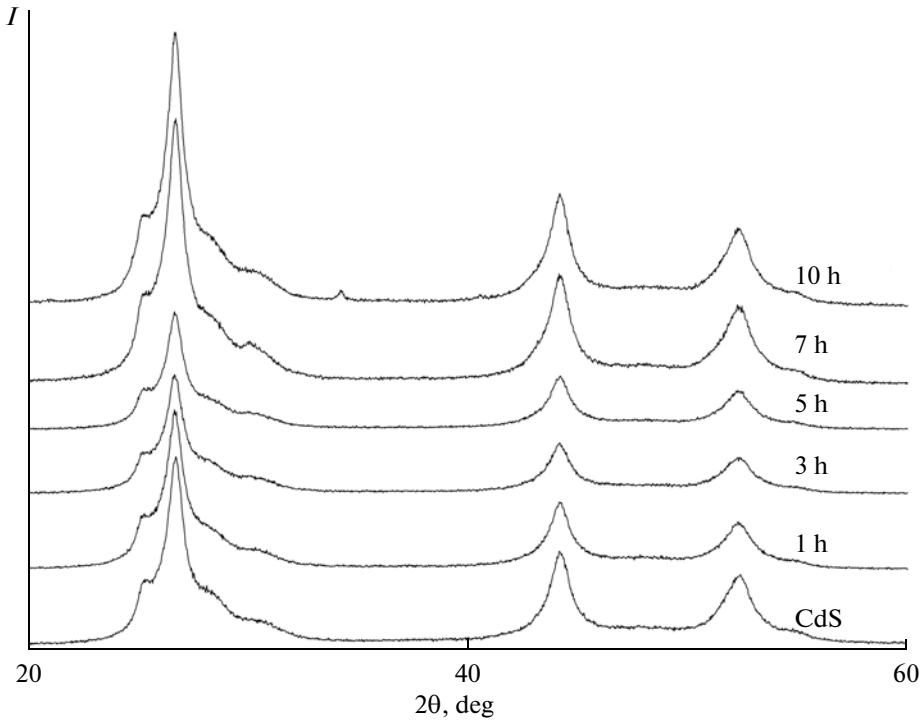

Fig. 1. X-ray diffraction patterns of nanocrystalline powders of as-deposited CdS and cadmium sulfide treated for 1, 3, 5, 7, and 10 h at 353 K in a citrate–ammonia solution of lead acetate.

electron microscopy with energy dispersive X-ray analysis, and thermal analysis.

To assess the thermal stability of an analyte, determine the transformation temperature, and study thermal events that occur during thermal annealing of a nanopowder, differential thermal analysis (DTA) and thermogravimetry (TG) were used.

The following analytical equipment was used: a Shimadzu XRD-7000 diffractometer (2θ = 20°–80°, step 0.03°, counting time 20 s per point, Cu$K_{\alpha 1,2}$ radiation), a Setaram SETSYS Evolution differential scanning calorimeter (DTA and DTG modes, at a heating rate of 10 K/min in a 20 mL/min argon flow), and a JEOL-JSM 6390 LA scanning electron microscope with a JED-2300 energy dispersive analyzer in backscattered and secondary electrons. X-ray powder diffraction patterns were interpreted with the PowderCell 2.4 program using ICCD cards.

The size of nanopowder particles was determined with the Measure program, and the size distribution was evaluated with the StatGraphics program.

RESULTS AND DISCUSSION

The phase composition and crystallographic characteristics were studied for both the as-deposited CdS powders and the powders modified by treatment in a citrate–ammonia solution of lead acetate and annealed in an argon atmosphere. Cadmium sulfide powders were used as starting materials.

Figure 1 shows the experimental X-ray diffraction patterns of the initial CdS nanopowder and modified CdS samples. The patterns have the same set of reflections. The strongest reflection is observed at 2θ = 26.8°, and two considerably weaker reflections are observed at ~44° and ~52°. A possible explanation of these diffraction patterns can be the formation of a mixture of crystallites of the cubic sphalerite phase with space group $F\bar{4}3m$ and the hexagonal wurtzite phase with space group $P6_3mc$. The crystallographic characteristics and the phase composition of freshly deposited and modified CdS powders as a function of the duration of the contact of cadmium sulfide with an aqueous lead acetate solution are summarized in the table.

The content of the low-temperature cubic sphalerite phase in modified cadmium sulfide nanopowders after treatment with a lead acetate solution ranges within 45.2–59.2 wt %. After the contact with a lead salt solution for 5 h, the unit cell parameter of the modified nanopowder increased from $a = 5.79 \pm 0.03$ Å, typical of the initial CdS nanopowder, to 5.82 ± 0.03 Å. Thus, we can assume that lead atoms were introduced into the metastable cubic structure of CdS.

As for the hexagonal wurtzite modification, its amount is comparable with that of the cubic phase and changes oppositely to the latter. The unit cell parameters of the wurtzite phase in modified CdS powders and initial cadmium sulfide sample remained almost unaltered: $a = 4.10 \pm 0.01$ Å, $c = 6.70 \pm 0.01$ Å.

Crystallographic characteristics and phase composition of as-deposited and modified CdS powders at different durations of contact of a CdS deposit with a citrate–ammonia solution of lead acetate before and after DTA

Time, h	CdS wurtzite structure (space group $P6_3mc$)			CdS sphalerite structure (space group $F\bar{4}3m$)	
	wt %	a, Å	c, Å	wt %	a, Å
0	41.7	4.10	6.70	58.3	5.79
1	54.8	4.10	6.70	45.2	5.80
3	50.8	4.10	6.70	49.2	5.81
5	50.0	4.09	6.70	50.0	5.80
6	40.8	4.10	6.70	59.2	5.82
7	45.6	4.09	6.70	54.4	5.79
10	45.5	4.10	6.70	55.5	5.79
Powder after DTA (20–600°C in an argon flow)					
0	100	4.135	6.712	–	–
1	98.8	4.134	6.710	–	–
3	97.0	4.132	6.706	–	–
5	98.5	4.133	6.708	–	–
6	96.8	4.132	6.706	–	–
7	97.5	4.132	6.708	–	–
10	93.7	4.134	6.710	–	–

The structures of modified CdS powders were refined with the PowderCell program package. To do this, models corresponding to space groups $F\bar{4}3m$ and $P6_3mc$ were used. Figure 2 shows the experimental (solid line) and theoretical (dotted line for the hexagonal phase and dashed and dotted line for the cubic phase) diffraction patterns of the CdS nanopowder modified by treatment for 5 h, as well as their superposition (dashed) and the difference curve. As seen in the figure, the superposition of the corresponding partial diffraction patterns satisfactorily fits the experimental diffraction pattern of the nanopowder.

Apart from the presence of different phases, the X-ray powder diffraction patterns did not show some lines (or they were rather weak) characteristic of the hexagonal CdS phase, for example (102) and (202), and of the cubic phase, (222). Analogous data for cadmium sulfide powders have been reported, for example, in [8]. At the same time, the diffraction patterns of both the initial CdS nanopowder and modified samples show a strong reflection ($2\theta = 28.6°$) responsible for orientation along the c axis, which is consistent with the data in [9, 10] for cadmium sulfide nanoparticles. This has been confirmed by transmission electron microscopy, revealing the orientation of hexagonal particles with $d = 0.359$ nm along the (001) axis. The particle size was 10–35 nm, and their agglomerates were 80–200 nm in size. It has been suggested to assign the nanophase to a polytype structure [11–13].

Relevant literature data [8–13] have been scrutinized in [14–16], and it has been suggested that a specific feature of the CdS structure in the nanosized state is disordered packing of atomic planes of nanoparticles. This conclusion is based on comparison of the experimental and theoretical diffraction patterns. It is worth noting that the program of calculation of diffraction patterns for CdS nanoparticles developed in [14–16] makes it possible to consider the effect of the powder particle size, shape, and boundary on the form of the diffraction pattern. At the same time, the crystal lattice of such a structure is described by space group $P6_3mc$, and the particles have a shape close to a hexagonal prism with the characteristic size of ~5 nm.

As in the above works, we revealed a mixture of the cubic and hexagonal phases of cadmium sulfide (table). Figure 2 shows a superposition of the respective partial diffraction patterns, which satisfactorily fits the experimental X-ray diffraction pattern of the powder compositions. Thus, comparison of the experimental diffraction patterns in [12] with those reported by us does not contradict the polytype structure of CdS crystals postulated in [12]. On the whole, the calculated diffraction patterns [14–16] are consistent with the experimental diffraction patterns recorded in the present study. As for the dominant growth direction along the c axis suggested in [9, 10], it is not confirmed under our experimental conditions.

According to X-ray diffraction [17], CdS nanoparticles synthesized in a high-pressure polyethylene matrix by means of thermal decomposition of the thiourea complex of cadmium acetate have a hexagonal structure. A hexagonal structure has also been found for cadmium sulfide nanoparticles produced

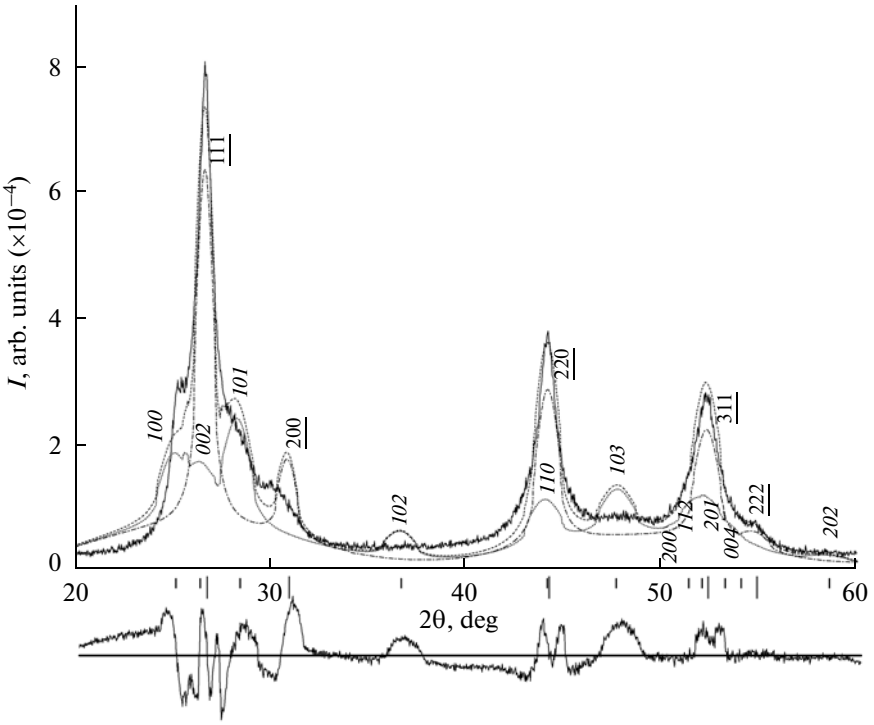

Fig. 2. Experimental (solid line) and theoretical (dotted for the hexagonal phase, dotted and dashed line for the cubic phase) X-ray diffraction patterns of a CdS nanopowder modified by treatment for 5 h with a citrate–ammonia solution of lead acetate, as well as their superposition (dashed line) and difference curve.

from cadmium pivalate and elemental sulfur dissolved in orthoxylene on heating (120°C) [18].

However, a metastable cubic phase has been revealed by X-ray diffraction in nanostructured CdS films deposited at room temperature from an aqueous solution containing cadmium sulfate, ammonia, and thiourea [19, 20]; commercially available cadmium sulfide powders [21]; and CdS nanoparticles synthesized by electrochemical deposition at 70°C in an ethylene glycol solution of elemental sulfur [22].

In our opinion, a decisive factor for formation of a definite structure of CdS nanopowders (hexagonal, cubic, a mixture of both modifications, or a disordered closely packed structure) is the formation rate of CdS nanoparticles. The chemical reaction between the cadmium complex ion CdL^{2+} and thiourea CSN_2H_4 in an alkaline solution can be presented as

$$CdL^{2+} + CSN_2H_4 + 2OH^- \rightarrow CdS + L + H_2CN_2 + 2H_2O,$$

where L is a complexing agent.

The formation rate of the solid cadmium sulfide phase is determined, first of all, by temperature, the composition and concentrations of the reaction mixture components, and the surface area of the forming particles.

At low reaction rates, cubic nanocrystals are formed; high rates of the reaction of the metal with the chalcogen lead to the formation of a hexagonal wurtzite structure.

Under conditions favorable for intermediate reaction rates, a solid phase containing both crystalline modifications can form [23], which was observed in our study.

It is known that the cubic CdS modification converts to the more stable hexagonal wurtzite structure in the temperature range 300–400°C [19, 24].

According to [11], the crystal structure also depends on the particle size: <4 nm, cubic structure; >6 nm, hexagonal lattice; 4–6 nm, polytype structure.

X-ray diffraction analysis of individual CdS and cadmium sulfide powders kept in a lead salt solution for 1, 3, 5, 7, or 10 h and then heated to 600°C in an argon flow revealed structures with a high degree of crystallinity. This is confirmed, in particular, by complete splitting of interferences into $K_{\alpha 1}$- and $K_{\alpha 2}$ doublets at large angles.

The PowderCell analysis of X-ray diffraction patterns showed that the samples mainly consist of the hexagonal CdS phase (space group $P6_3mc$). It is worth noting that Frenkel pairs $Cd^{\bullet}I$–v'Cd form in CdS films at moderate temperatures, and their formation is a thermally activated process accompanied by the displacement of atoms in the crystal structure upon the phase transition of the metastable cubic CdS modification to the stable hexagonal modification [25]. For the CdS samples kept in a lead salt solution, the *a* and

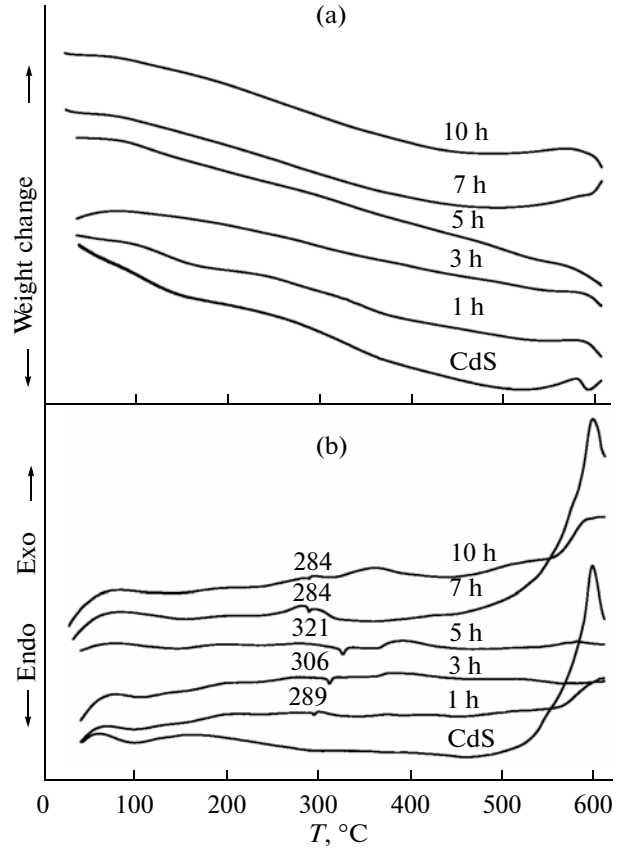

Fig. 3. (a) TG and (b) DTA curves of the initial and modified CdS powders with endotherm temperatures. Powders were modified by keeping them for 1–10 h in a citrate–ammonia solution of lead acetate.

c unit cell parameters somewhat differ from the unit cell parameters of both the initial CdS sample and analogous non-heat-treated samples (table). This can be evidence of the change in the crystal phase composition, in particular, due to the endocrypty playing a crucial role for incompatible elements [7] with limited isomorphic capabilities. At the same time, the substitution of lead ions for cadmium ions in the surface layers of cadmium sulfide nanoparticles cannot be ruled out.

It has been determined that modified nanopowders after heat treatment contain 1.1–3.9 wt % $PbSO_4$ (space group *Pnma*) and 0.4–1.2 wt % CdO inclusions (space group $Fm\bar{3}m$). The unit cell parameters of these phases are, respectively, $a = 8.467 \pm 0.66$ Å, $b = 5.394 \pm 0.011$ Å, $c = 6.946 \pm 0.086$ and 4.693 ± 0.002 Å. The content of the lead sulfate phase clearly tends to increase with an increase in the time of contact of CdS nanopowders with a lead salt solution.

It should be noted that, for the hexagonal structure, the *a* and *c* unit cell parameters of the Cd–Pb–S composition are maximal at a contact time of 1 and 10 h and minimal at a contact time of 5 and 6 h.

It is known [26, 27] that, even at moderate temperatures, structural and phase transformation in nanocrystalline metal sulfide powders are accompanied by oxidation yielding oxide and sulfate phases. The source of oxygen for oxidation can be impurities of oxygen containing compounds (basic salts and cadmium hydroxide) introduced into the initial CdS powder during its chemical deposition. In particular, the formation of the $Cd(OH)_2$ impurity in the reaction mixture has been supported by our calculations of ionic equilibria [28]. We believe that, in the presence of these oxygen-containing phases, the formation of lead sulfate and cadmium oxide in Cd–Pb–S powders heated to 600°C cannot be ruled out even in an argon atmosphere:

$$Cd–Pb–S + 5/2O_2 = CdO + PbSO_4.$$

The available crystallographic data are insufficient to verify the formation and composition of the substitutional solid solution $Cd_{1-x}Pb_xS$, and additional studies, in particular, by the TEM method, are required.

Thermal events during thermal annealing of modified sulfide nanopowders were studied by TGA (Fig. 3a) and DTA (Fig. 3b). As follows from Fig. 3b, the thermoanalytical curves show a strong endotherm in the temperature range 284–321°C. Its position depends on the duration of treatment of the CdS powder with an aqueous lead salt solution. The endotherm in this temperature range has been reported for chemically deposited cadmium sulfide films and powders [19, 20]. The maximal temperature of the endotherm 321°C is observed for the nanopowder treated with an aqueous lead acetate solution for 5 h. The thermoanalytical curve of the individual CdS has no a similar endotherm. Likewise, it was not observed in [29]. However, the phase diagram of individual CdS has a line of polymorphic transformation at 321°C [30]. We may assume that the endotherm for the initial and modified cadmium sulfide samples is caused by the transformation of the structure from the unstable (cubic) modification to the stable (hexagonal) polymorph, which is catalyzed by the lead in the surface layers of the nanopowder. The decrease in the endotherm temperature at contact times longer than 5 h can be explained by some loosening of the material structure induced by solvation and high content of ligands in solution.

At temperatures 500–600°C, the DTA curves of Cd–Pb–S powders show an exotherm. For the CdS sample treated for 7 h with an aqueous lead acetate solution and for the initial CdS sample, the exotherm intensity is maximal. In the TG curves, this exotherm corresponds to some weight loss and then to a small weight gain. This event can be attributed to the coarsening of nanopowder particles [31] accompanied by the phase transition to the hexagonal structure, which is confirmed above by X-ray diffraction analysis. It has been reported that annealing at 520–560°C not only leads to coarsening of crystals on the surface of samples containing 90 wt % CdS and 10 wt % PbS but also

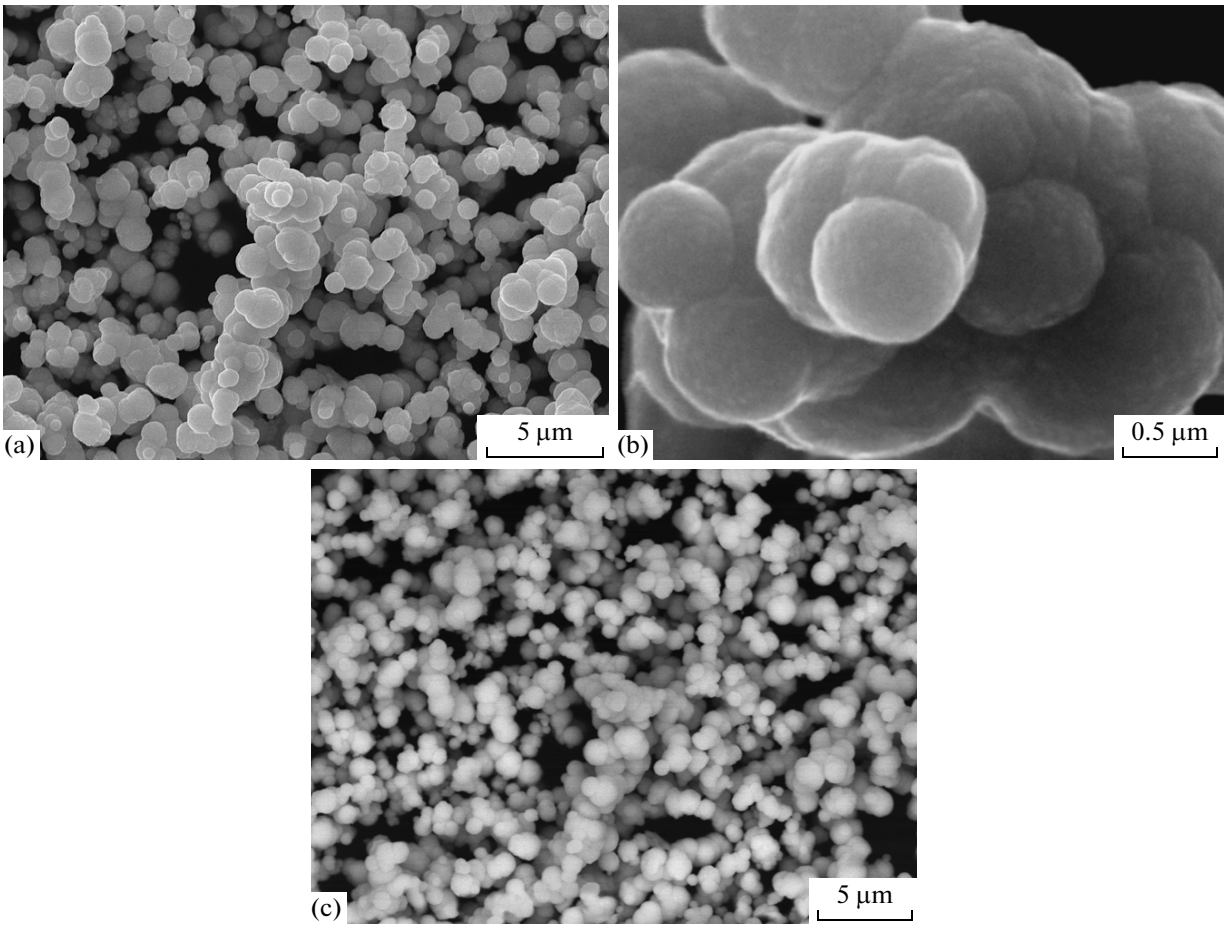

Fig. 4. Electron microscopy images of Cd–Pb–S nanopowders (a, b) after heating to 350°C and (c) the same in the phase contrast mode.

activates diffusion and formation of the $Pb_xCd_{1-x}S$ solid solution [3].

Electron microscopy studies of the microstructure of CdS particles treated with an aqueous solution of lead acetate for 5 h after heating to 350°C demonstrated that at ×5000 magnification they are spherical agglomerates with an average size of ~1 μm (Fig. 4a). However, at ×40000 magnification, it is seen that these agglomerates are formed by particles 30–40 nm in size (Fig. 4b). Studies of Cd–Pb–S nanopowder particles in the phase contrast mode (Fig. 4c) reveals relatively high phase homogeneity of their surface regions. In this context, it can be assumed that ion exchange in the surface layers of Cd–Pb–S compositions leads to formation of the $Pb_xCd_{1-x}S$ solid solution.

Thus, CdS nanopowders chemically deposited and modified by treating for 1–10 h with an aqueous lead acetate solution have been studied by X-ray diffraction, electron microscopy, DTA and TG.

The content of crystalline modifications of wurtzite and sphalerite in nanopowder compositions based on cadmium sulfide was found to correlate with the conditions of their synthesis.

According to DTA and TG, the Cd–Pb–S nanopowders have a pronounced endotherm in the temperature range 284–321°C, and its position depends of the duration of contact of the CdS powder with an aqueous lead salt solution. According to X-ray diffraction, after heating to 600°C, modified CdS samples contain, respectively, 1.1–3.9 and 0.4–2.4 wt % of crystalline phases of lead sulfate and cadmium oxide.

X-ray diffraction and electron microscopy studies of nanopowders enable the assumption that ion exchange in the surface layer of CdS particles contacting with a citrate–ammonia solution of lead acetate results in formation of the $Pb_xCd_{1-x}S$ solid solution phase.

REFERENCES

1. A. G. Rokakh and N. B. Trofimova, Zh. Tekh. Fiz. **71** (7), 140 (2001).
2. S. V. Stetsyura, I. V. Malyar, A. A. Serdobintsev, and S. A. Klimova, Fiz. Tekhn. Poluprovodnikov **43**, 1102 (2009).
3. S. V. Stetsyura and I. V. Malyar, Fiz. Tekhn. Poluprovodnikov **45**, 916 (2011).

4. P. M. Behtke and P. B. Barton, Am. Mineral. **56**, 2034 (1971).
5. A. G. Rokakh, S. V. Stetsyura, A. G. Zhukov, and A. A. Serdobintsev, Tech. Phys. Lett. **32**, 30 (2006).
6. V. F. Markov, N. A. Forostyanaya, A. N. Ermakov, and L. N. Maskaeva, Butlerovsk. Soobshch. **27** (16), 56 (2011).
7. V. L. Tauson, N. V. Smagunov, V. A. Datkov, and T. M. Pastushkova, Geochem. Int. **45**, 1146 (2007).
8. O. Conde, A. G. Rolo, M. J. M. Gomes, et al., J. Crystal Growth **247**, 371(2003).
9. B. Su, M. Wei, and K. L. Choy, Mater. Lett. **47**, 83 (2001).
10. K. Senthil, D. Mangalaraj, Sa. K. Narayandass, et al., Physica B: Condens. Matter **304**, 175 (2001).
11. C. Ricolleau, L. Audinet, M. Gandais, and T. Gacoin, Thin Solid Films **336**, 213 (1998).
12. P. N. Gibson, M. E. Ozsan, D. Lincot, et al., Thin Solid Films **361–362**, 34 (2000).
13. H. El Malikia, J. C. Bernedea, S. Marsillaca, et al., Appl. Surf. Sci. **205**, 65 (2003).
14. A. S. Vorokh, Extended Abstract of Candidate's Dissertation in Mathematical Physics (Yekaterinburg, 2009).
15. A. S. Vorokh and A. A. Rempel', Phys. Solid State **49**, 148 (2007).
16. A. S. Vorokh and A. A. Rempel', Dokl. Phys. **52**, 200 (2007).
17. V. I. Kochubei, D. I. Kochubei, Yu. G. Konyukhova, and I. V. Zabenkov, Poverkhnost. Rentgen., Sinkhrotron. Neitron. Issled., No. 8, 40 (2010).
18. E. K. Volkova and V. I. Kochubei, Izv. Samarsk. Nauch. Tsentra RAN **14** (4), 113 (2010).
19. S. A. Gavrilov, A. A. Sherchenkov, A. B. Apal'kov, et al., Ros. Nanotekhnol. **1**, 228 (2006).
20. G. I. Grin', A. M. Pancheva, P. A. Kozub, et al., Vopr. Khim. Khim. Tekhnol., No. 4, 149 (2009).
21. I. Kh. Akopyan, T. I. Ivanova, M. E. Labzovskaya, et al., Tech. Phys. Lett. **36**, 240 (2010).
22. Y. L. Yang, L. Y. He, and H. Xiang, Russ. J. Electrochem. **42**, 954 (2006).
23. N. G. Piven, L. P. Shcherbak, P. I. Feichuk, et al., Kondens. Sredy Mezhfaz. Granitsy **8**, 315 (2006).
24. A. Cortes, H. Gomez, G. Riveros, et al., Solar Energy Mater. Solar Cells **82**, 21 (2004).
25. R. Lozada-Morales, O. Zelaya-Angel, and G. Torres-Delgado, Appl. Surf. Sci. **175–176**, 562 (2001).
26. H. El Malikia, J. C. Bernedea, S. Marsillaca, et al., Appl. Surf. Sci. **205**, 65 (2003).
27. S. B. Qadri, A. Singh, and M. Yousuf, Thin Solid Films **432**, 506 (2003).
28. V. F. Markov and L. N. Maskaeva, Russ. J. Phys. Chem. A **84**, 1288 (2010).
29. R. I. Dimitrov and B. S. Boyanov, J. Therm. Anal. Calorim. **61**, 181 (2000).
30. *Phase Diagrams of Binary Metal Systems, A Handbook*, Ed. by N. P. Lyakishev (Mashinostroenie, Moscow, 1996) [in Russian].
31. V. P. Egunov, *Introduction to Thermal Analysis* (PO SamVen, Samara, 1996) [in Russian].

Translated by G. Kirakosyan